



# Short-term and long-term effects of osteoporosis on incisor teeth and femoral bones evaluated by Raman spectroscopy and energy dispersive X-ray analysis in ovariectomized rats

Fernanda Rossi Paolillo<sup>1</sup> · Renan Arnon Romano<sup>1</sup> · Luciana de Matos<sup>1</sup> · Airton Abrahão Martin<sup>2,3</sup> · Francisco Eduardo Gontijo Guimarães<sup>1</sup> · Jarbas Caiado de Castro Neto<sup>1</sup> · Vanderlei Salvador Bagnato<sup>1</sup>

Received: 9 August 2017 / Accepted: 4 January 2018 / Published online: 17 January 2018  
© The Japanese Society for Bone and Mineral Research and Springer Japan KK, part of Springer Nature 2018

## Abstract

There are few published data on the relationship between loss of bone mass due to osteoporosis and poor tooth quality. This study analyzed the effects of osteoporosis on incisor teeth and femoral bones using optical techniques in rats. Twenty female Wistar rats aged 6 months ( $n = 20$ ) were randomized into two groups: control group, non-ovariectomized rats ( $n = 10$ ); ovariectomy group, ovariectomized rats to induce osteoporosis ( $n = 10$ ). Each group was subdivided randomly into two groups containing five rats each as follows. Control group 1: non-ovariectomized rats euthanized at the age of 9 or 3 months post-ovariectomy ( $n = 5$ ); Control group 2: non-ovariectomized rats euthanized at the age of 1 year or 6 months post-ovariectomy ( $n = 5$ ); ovariectomy group 1: ovariectomized rats euthanized at the age of 9 months or 3 months post-ovariectomy ( $n = 5$ ); ovariectomy group 2: ovariectomized rats euthanized at the age of 1 year or 6 months post-ovariectomy ( $n = 5$ ). The incisor teeth and femoral bones of Wistar rats were removed to perform Raman spectroscopy using an excitation laser at 785 nm. In addition, an energy-dispersive X-ray spectrometer system was used to evaluate calcium (Ca) and phosphorus (P). The main findings included significant changes ( $p < 0.05$ ) for phosphate and carbonate band areas for both incisor teeth and femur bones. In addition, there was significant negative correlation between the P concentration and phosphate/carbonate ratio (lower P content–larger ratio,  $p < 0.05$ ) for incisor teeth and femoral bones. The proline and  $\text{CH}_2$  wag band areas were significantly reduced only for the incisor teeth ( $p < 0.05$ ). Therefore, Raman spectroscopy assessed the compositional, physicochemical and structural changes in hard tissue. The current study also pointed out the possible action mechanisms of these changes, bone fracture risk and dental fragility. It is important to emphasize that poor dental quality may also occur due to osteoporosis.

**Keywords** Raman spectroscopy · EDX · Tooth · Bone · Osteoporosis

## Introduction

Optical spectroscopy is a non-destructive and precise method, which can be used as a potential tool for diagnosis [1, 2]. The main characteristic is the study of the interaction between light and electrons of atoms and molecules of biological tissue. In particular, the Raman effect is characterized by promoting molecular vibrations through inelastic scattering of monochromatic laser photons. Inelastic scattering occurs when the scattered light has a frequency different from that of incident light with the remaining energy coupled to vibration. It provides a molecular fingerprint of the analyzed biological sample because each Raman spectral band is specific to a particular chemical group [1, 2]. The obtained spectrum is characterized by shifts in wavenumbers (inverse

✉ Fernanda Rossi Paolillo  
fer.nanda.rp@hotmail.com

<sup>1</sup> Optics Group from São Carlos Institute of Physics (IFSC), University of São Paulo (USP), Av. Trabalhador São-carlense, 400, Centro, São Carlos, SP CEP 13560-970, Brazil

<sup>2</sup> Department of Physics from Federal University of Piauí (UFPI), Campus Universitário Ministro Petrônio Portella, Bairro Ininga, Teresina, Bairro Ininga, Teresina PI 64049-550, Brazil

<sup>3</sup> Department of Biomedical Engineering from Brazil University (UnBr), Rua Carolina Fonseca, 584, Itaquera, SP, Brazil

of wavelength in  $\text{cm}^{-1}$ ) from the incident frequency. For hard tissue, the main vibrational bands and their respective wavenumber range for bone and dentin are  $\nu_2\text{PO}_4^{3-}$  (422–454  $\text{cm}^{-1}$ ),  $\nu_4\text{PO}_4^{3-}$  (578–617  $\text{cm}^{-1}$ ), C–C stretching (815–921  $\text{cm}^{-1}$ ),  $\nu_1\text{PO}_4^{3-}$  (957–962  $\text{cm}^{-1}$ ),  $\text{HPO}_4^{2-}$  (1003–1005  $\text{cm}^{-1}$ ),  $\nu_1\text{PO}_4^{3-}$  (1003–1005  $\text{cm}^{-1}$ ),  $\nu_1\text{CO}_3^{2-}$  (860–890  $\text{cm}^{-1}$ ), amide III (1243–1269  $\text{cm}^{-1}$ ),  $\text{CH}_2$  wag (1447–1452  $\text{cm}^{-1}$ ), amide II (1240–1580  $\text{cm}^{-1}$ ) and amide I (1595–1720  $\text{cm}^{-1}$ ). Regarding the enamel, it is similar to bone and dentin, however there were no amide Raman bands because enamel is a very hard tissue with mostly mineral composition ( $\sim 96\%$  mineral content) [3].

Hard tissue evaluated by Raman spectroscopy has been used to analyze fossils [4], embalmed subjects [5], cadavers [6], animals [7] and for clinical trials [8]. The main components of hard tissue analyzed by Raman Spectroscopy are phosphate, carbonate and matrix collagen.

Bone and dentin are composite structures that consist of apatite crystals deposited in an orderly fashion on an organic matrix consisting of non-collagenous proteins and collagen, predominantly type I [4]. Odontoblasts and osteoblasts are cells whose biological functions are, respectively, dentinogenesis and osteogenesis for formation of mineralized tissue [9] while osteoclast and odontoclast show a similar regulatory mechanism of mineralized tissue resorption. This mechanism is complex and correlated for permanent teeth eruption, root resorption or craniofacial anomalies [10].

Concerning the dentin of the ovariectomized rats, Yokose et al. [11] found smaller dentinogenic capacity and reduced mineralization in incisor odontoblasts due to estrogen deficiency, although the mechanisms are still poorly understood. These authors also found increased glycosylation of proteoglycan in predentin which may influence the metabolism of odontoblasts [11]. Kim et al. [12] showed that low levels of osteonectin were found in predentin, indicating lower protein content in ovariectomized rats. In addition, a lack of calcification and/or enhanced formation of predentin by odontoblasts lead to thickening of the predentin area. This suggests that the predentin has metabolic effects as an osteoid in bone [12]. Some studies also found reduced expression of odontoblast/osteoblast markers in the incisors of ovariectomized rats which affect the mineralization, dentinogenesis and compressive strength [13–15].

Several studies [16, 17] have been carried out using rat incisor teeth because the molars are permanent teeth that erupt during the first weeks after birth and never grow continuously; therefore, they clearly show marked oral environment- and age-dependent changes due to static aspects. Differently, rat incisors are a dynamic system, which shows continuous eruption, growth, calcification, attrition and wearing loss throughout the life of the rodents. This cycle is in equilibrium under normal conditions. Therefore, systemic disturbances

in mineral metabolism such as osteoporosis may affect odontogenesis.

Osteoporosis is a systemic disease which generates a disruption of inorganic ion homeostasis and leads to a reduction in the calcium and phosphorus levels, changing the mineralization process of teeth and bones [13, 18, 19]. Demineralization of teeth, as well as the loss of bone mass and microarchitectural deterioration result in changes in non-collagenous proteins, weakening teeth and bones [13, 18]. Few studies have correlated the loss of bone mass due to osteoporosis with poor tooth quality [13–15, 19]. The key to this problem is that a lack of estrogen accelerates the development of osteoporosis for both type 1 (postmenopausal) and type 2 (senile) [20]. In this context, various studies have been carried out using ovariectomized rats [14], postmenopausal women and elderly people [21].

A previous study from our group [19] has demonstrated that demineralization leading to changes in hard tissue was evaluated by fluorescence spectroscopy using the excitation laser at 532 nm. Moreover, these results suggested that osteoporosis may affect both the teeth and bones in rats. Other studies with ovariectomized rats showed a mineralization deficit and impaired regeneration of incisors [15] and jaws [13].

A clinical trial was performed on fractured and non-fractured postmenopausal women and revealed that the Raman spectroscopy of bone biopsies was significantly different between the groups, indicating that a change in the chemical composition was associated with an occurrence of osteoporotic fracture [22]. Another study using Raman spectroscopy in the murine model of arthritis with secondary osteoporosis showed that mineralization quality and bone collagen can predict fractures [23].

In this context, Raman spectroscopy, used to assess systemic changes, such as osteoporosis via hard tissues (teeth and bones) has not been widely investigated.

The aim of the current study was to investigate the short- and long-term effects of osteoporosis on incisor teeth and femur bones evaluated by Raman spectroscopy and energy-dispersive X-ray (EDX) spectrometer in ovariectomized rats. Our hypothesis was that Raman spectroscopy may assess changes in hard tissue at the molecular level for compositional, physicochemical and structural analysis due to systemic disturbances in mineral metabolism.

## Materials and methods

This study was approved by the ethics committee of the São Carlos Institute of Physics (IFSC), University of São Paulo (USP) in São Carlos, Brazil (number 08/2014). All animal procedures were performed according to the principles in the Guide for the Care and Use of Laboratory Animals.

## Animal care and experimental groups

Twenty female Wistar rats (body mass 400–500 g) were kept in a cage with food and water ad libitum on a 12:12-h light–dark cycle at  $23 \pm 1$  °C. The animals aged 6 months ( $n = 20$ ) were randomized into two groups: control group (C): non-ovariectomized rats ( $n = 10$ ); ovariectomy group (OV): ovariectomized rats to induce osteoporosis ( $n = 10$ ). Each group was subdivided randomly into two groups containing five rats each. Control group 1 (C1): non-ovariectomized rats euthanized at the age of 9 months or 3 months post-ovariectomy ( $n = 5$ ); control group 2 (C2): non-ovariectomized rats euthanized at the age of 1 year or 6 months post-ovariectomy ( $n = 5$ ); ovariectomy group 1 (OV1): ovariectomized rats euthanized at the age of 9 or 3 months post-ovariectomy ( $n = 5$ ); ovariectomy group 2 (OV2): ovariectomized rats euthanized at the age of 1 year or 6 months post-ovariectomy ( $n = 5$ ). The time line of experimental procedure can be seen in Fig. 1.

The ovariectomy was performed as previously described [19]. The animals were anaesthetized using an intraperitoneal injection of 2% xylazine (Bayer, São Paulo, Brazil)

(12 mg/kg) and 10% ketamine (Agener União, Brasília, Brazil) (80 mg/kg). Bilateral ovariectomy was performed via translumbar incisions. The uterine tubes were ligated (catgut 4.0) and the ovaries were removed. The rats were euthanized by intraperitoneal administration of excess anesthetic (10/180 mg/kg xylazine/ketamine) for ex vivo analysis. Immediately thereafter, the lower incisor teeth and the femur bones (entire samples) were removed, cleaned, embedded in physiological saline solution and frozen in sealed plastic tubes at  $-20$  °C [24]. All samples of lower right incisors ( $n = 20$ ) and right femurs ( $n = 20$ ) from all animals ( $n = 20$ ) were utilized for all experiments (Raman spectroscopy and EDX). For Raman spectroscopy, entire samples were used. Afterwards, for EDX, sample preparation was necessary prior to measurement.

## Raman spectroscopy

The portable Raman spectrometry system (Ocean Optics, Inc., Dunedin, FL, USA) consists of a spectrometer and a diode laser (785 nm) for excitation with spectral resolution of  $11 \text{ cm}^{-1}$ . The probe was perpendicularly placed on the incisor teeth and femur bones (trochanteric region). The

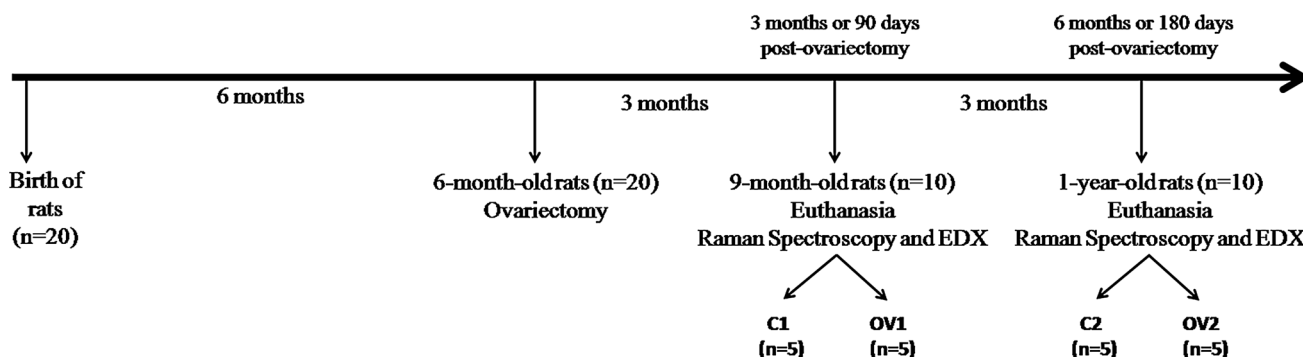


Fig. 1 Timeline of the experimental procedure

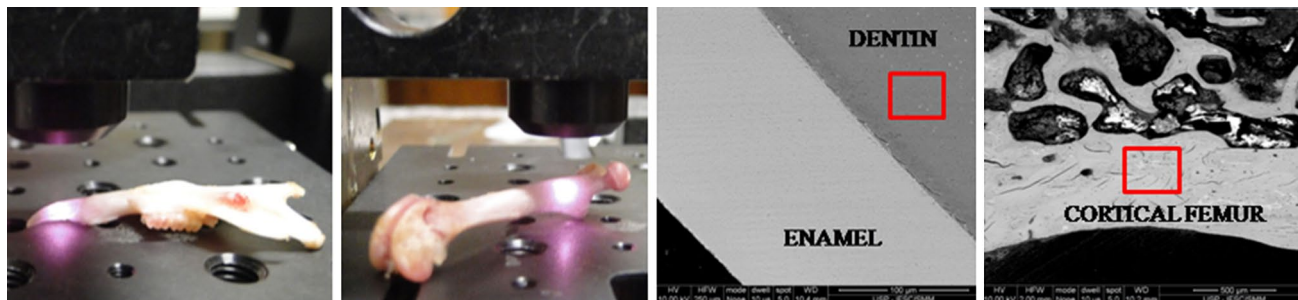
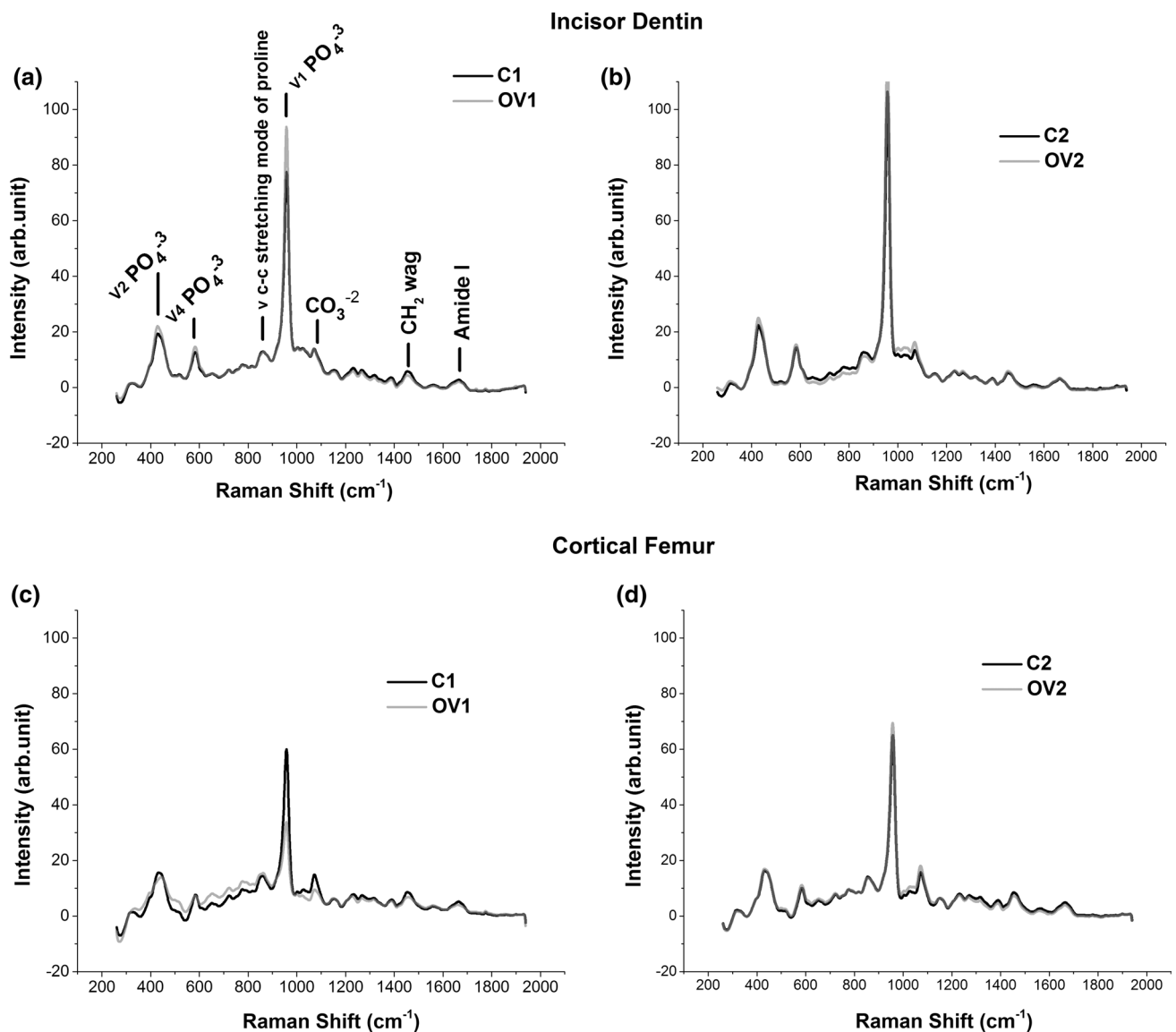


Fig. 2 Tissue samples during experimental procedure. A single spectra was collected from all the samples [incisors ( $n = 20$ ) and femurs ( $n = 20$ )] for Raman Spectroscopy. Following description proceeds, the tissue location (incisor dentin and cortical femur) from the longitudinally cut samples to perform an energy dispersive X-ray (EDX)

measurement corresponding to scanning electron microscopy images. The concentrations of Ca and P were measured by randomly selecting three different points in the featured area from all samples [incisors ( $n = 20$ ) and femurs ( $n = 20$ )]



**Fig. 3** Raman spectra of incisor dentin (a, b) and cortical femur (c, d) for control group (C1 and C2) and ovariectomized rats (OV1 and OV2) corresponding to different times of the year (3 and 6 months post-ovariectomy, respectively, numbers 1 and 2). Data represents the mean values of band intensity (arbitrary units) as a function of

Raman Shift (wavenumbers,  $\text{cm}^{-1}$ ) for each group. The first graph illustrates the analyzed bands for all samples: phosphate [ ${}_{\nu_1}\text{PO}_4^{3-}$  ( $960\text{ cm}^{-1}$ );  ${}_{\nu_2}\text{PO}_4^{3-}$  ( $430\text{ cm}^{-1}$ ) and  ${}_{\nu_4}\text{PO}_4^{3-}$  ( $580\text{ cm}^{-1}$ )], carbonate [ $\text{CO}_3^{2-}$  ( $1070\text{ cm}^{-1}$ )], amide I ( $1658\text{ cm}^{-1}$ ),  $\nu\text{C}-\text{C}$  stretching mode of proline ( $854\text{ cm}^{-1}$ ) and  $\text{CH}_2$  wag ( $1446\text{ cm}^{-1}$ )

laser power average was 130 mW at the samples, obtaining a Raman signal with good signal-to-noise ratio without heating. Single spectra between 400 and  $1800\text{ cm}^{-1}$  was collected with an approximate 1 cm distance between the probe and the samples to provide an appropriate focus (Fig. 2). The optical way was fixed and the focal adjustment was made to ensure Raman maximum intensity. The integration time was 10 s and 3 accumulations were performed. Single spectra was collected because this portable system does not measure point by point (laser scanning mode). This portable system is not a confocal Raman microscope. Therefore, in the current study, the

illuminated area of the sample is relatively large compared with a confocal Raman microscope. Moreover, this portable Raman spectrometry system does not reconstruct images from the Raman band. The data acquisition was performed in the dark and the SpectraSuite® software (Ocean Optics, Inc., Dunedin, FL, USA) was used. For data analysis, the correction of the baseline by quadratic function was performed. Subsequently, the normalization of the spectrum by the area was performed.

The vibration bands analyzed (Fig. 3) were phosphate [ ${}_{\nu_1}\text{PO}_4^{3-}$  ( $960\text{ cm}^{-1}$ );  ${}_{\nu_2}\text{PO}_4^{3-}$  ( $430\text{ cm}^{-1}$ ) and  ${}_{\nu_4}\text{PO}_4^{3-}$  ( $580\text{ cm}^{-1}$ )], carbonate [ $\text{CO}_3^{2-}$  ( $1070\text{ cm}^{-1}$ )],

**Table 1** Values of mean, standard deviation and statistical results of Raman shift band area

	Incisor dentin ( <i>n</i> = 20)				Cortical femur ( <i>n</i> = 20)			
	C1	OV1	C2	OV2	C1	OV1	C2	OV2
Raman shift (cm <sup>-1</sup> )								
430	1621 ± 99	1637 ± 63	1416 ± 140 <sup>b</sup>	1466 ± 113	1413 ± 80	1690 ± 329	1143 ± 80	1216 ± 82
580	434 ± 57	476 ± 275	498 ± 130	575 ± 129	113 ± 44	43 ± 28 <sup>a</sup>	194 ± 28	222 ± 45 <sup>c</sup>
854	1090 ± 187	1440 ± 270	875 ± 299	964 ± 455 <sup>c</sup>	1443 ± 143	1453 ± 324	1065 ± 243	1188 ± 275
960	2748 ± 137	3179 ± 966	3281 ± 423	3799 ± 490	2133 ± 386	1205 ± 336 <sup>a</sup>	2135 ± 103	2348 ± 352 <sup>c</sup>
1070	1297 ± 222	2057 ± 349	565 ± 248 <sup>b</sup>	1153 ± 469 <sup>c</sup>	816 ± 406	704 ± 468	555 ± 189	1104 ± 517
1446	167 ± 47	124 ± 52 <sup>a</sup>	180 ± 53	203 ± 74	323 ± 48	264 ± 97	293 ± 60	270 ± 52
1658	63 ± 30	124 ± 52	96 ± 33	117 ± 76	211 ± 88	201 ± 226	154 ± 36	120 ± 39
Ratio								
430/1658	32 ± 17	54 ± 47	17 ± 9	19 ± 14	7 ± 16	18 ± 16	8 ± 2	12 ± 7
580/1658	9 ± 5	11 ± 6	6 ± 4	8 ± 6	0.71 ± 0.61	0.71 ± 0.98	1.29 ± 0.25	2.04 ± 0.86 <sup>a,b,c</sup>
960/1658	53 ± 27	86 ± 34 <sup>a</sup>	40 ± 23	49 ± 35 <sup>c</sup>	13 ± 8	15 ± 14	15 ± 4	22 ± 8
1070/430	0.81 ± 0.17	1.25 ± 0.19 <sup>a</sup>	0.39 ± 0.15 <sup>b</sup>	0.77 ± 0.28 <sup>a,c</sup>	0.63 ± 0.37	0.47 ± 0.38	0.49 ± 0.25	0.89 ± 0.37 <sup>a,c</sup>

Significant difference compared with C (a OV1 vs. C1 and OV2 vs. C2,  $p < 0.05$ ). Significant difference compared with C1 (b C2 vs. C1 and OV2 vs. C1,  $p < 0.05$ ); Significant difference compared with OV1 (c OV2 vs. OV1,  $p < 0.05$ )

C control group, C1 non-ovariectomized rats euthanized at the age of 9 months or 3 months post-ovariectomy, C2 non-ovariectomized rats euthanized at the age of 1 year or 6 months post-ovariectomy, OV ovariectomized group, OV1 ovariectomized rats euthanized at the age of 9 months or 3 months post-ovariectomy, OV2 ovariectomized rats euthanized at the age of 1 year or 6 months post-ovariectomy

amide I (1658 cm<sup>-1</sup>),  $\nu$  C–C stretching mode of proline (854 cm<sup>-1</sup>) and CH<sub>2</sub> wag (1446 cm<sup>-1</sup>) as well as phosphate to amide ratio [ $\nu_1$ PO<sub>4</sub><sup>3-</sup>/amide I (960/1658),  $\nu_2$ PO<sub>4</sub><sup>3-</sup>/amide I (430/1658)] and  $\nu_4$ PO<sub>4</sub><sup>3-</sup>/amide I ratio (580/1658)] and carbonate to phosphate ratio [CO<sub>3</sub><sup>2-</sup>/ $\nu_2$ PO<sub>4</sub><sup>3-</sup> (1070/430)].

### Energy-dispersive X-ray (EDX)

The samples were embedded by epoxy resin, longitudinally cut and polished. In addition, the samples were covered with carbon in order to ensure electrical conductivity during data acquisition. The atomic concentrations of elements of the incisor dentin and cortical femur, such as calcium (Ca) and phosphorus (P), were measured using energy-dispersive X-ray (EDX) spectrometry (Apollo X, EDAX Inc., Mahwah, NJ, USA). The spectrometer was attached to a computer system for data acquisition and processed using the EDAX's TEAM™ EDS Analysis System software (EDAX Inc., Mahwah, NJ, USA). The concentrations of Ca and P were measured by randomly selecting three different points in featured areas of the dentin and cortical femur (Fig. 2) from each specimen and calculating the mean of the each component and Ca/P ratio.

### Statistical analysis

Measurements were shown by mean and standard deviations. The statistical analysis was made as previously described [25]. The Shapiro–Wilk and Levene tests were used to analyze the normality and homogeneity of variance. The

two-way analysis of variance (ANOVA) and Tukey's post hoc test were used for the ex vivo study of the Raman spectroscopy and EDX analysis. To investigate the relationship between the key variables, the Pearson product–moment correlation coefficients were used. Statistica for Windows Release 7 software (Statsoft Inc., Tulsa, OK, USA) was used for the statistical analysis and the significance level was set at 5% ( $p < 0.05$ ).

### Results

The Raman spectra for all the groups can be seen in Fig. 3. The data of the Raman shift band area is shown in Table 1.

For the incisor teeth, there were significant reductions ( $p < 0.05$ ) of: phosphate  $\nu_2$  (430 cm<sup>-1</sup>) band area for C2 compared with C1; phosphate  $\nu_4$  (580 cm<sup>-1</sup>) band area for OV1 compared with C1; CH<sub>2</sub> wag (1446 cm<sup>-1</sup>) band area for OV1 compared with C1; proline (854 cm<sup>-1</sup>) band area for OV2 compared with OV1 and; carbonate (1070 cm<sup>-1</sup>) band area for both groups C2 compared with C1 and, OV2 compared with OV1. For the femur bones, interestingly, the phosphate  $\nu_4$  (580 cm<sup>-1</sup>) and  $\nu_1$  (960 cm<sup>-1</sup>) band areas showed a significant reduction ( $p < 0.05$ ) in OV1 compared with C1; however, they significantly increased ( $p < 0.05$ ) in OV2 than OV1.

There was no significant result for the phosphate/amide ratio [ $\nu_2$ PO<sub>4</sub><sup>3-</sup>/Amide I (430/1658)], however there were significant results ( $p < 0.05$ ) for other phosphate/amide ratios



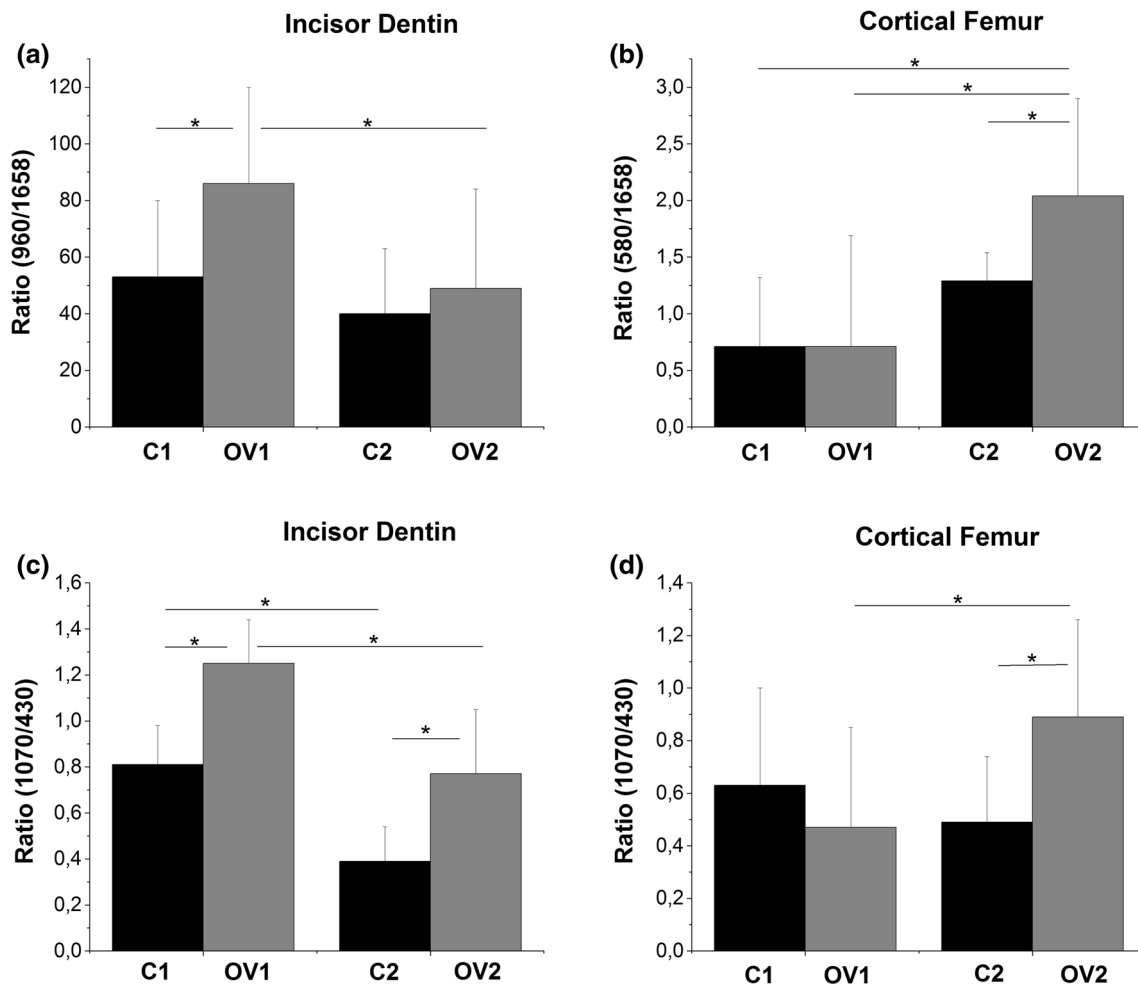


**Fig. 4** Phosphate/amide I ratio for incisor dentin (a) and cortical femur (b), as well as carbonate/phosphate ratio for incisor dentin (c) and cortical femur (d). For the incisor dentin, there was a higher 960/1658 ratio for OV1 vs. C1 and OV2 ( $p < 0.05$ ) and there was a significant increase in the 1070/430 ratio for OV1 vs. C1, C2 and

OV2, as well as for OV2 vs. C2 ( $p < 0.05$ ). However, there were significant reductions of the 1070/430 ratio for C2 vs. C1 and OV2 vs. OV1 ( $p < 0.05$ ). For the bones, there was a higher 580/1658 ratio for OV2 vs. C1, C2 and OV1. Moreover, the 1070/430 ratio was significantly greater for OV2 vs. C2 and OV1 ( $p < 0.05$ )

for both incisor teeth [ $\nu_1\text{PO}_4^{3-}/\text{Amida I}$  (960/1658)] and femur bones [ $\nu_4\text{PO}_4^{3-}/\text{Amida I}$  (580/1658)]. These significant results for incisor teeth and femur bones are also illustrated, respectively, in Fig. 4a, b. For the incisor teeth, there was a higher 960/1658 ratio for OV1 compared with groups C1 and OV2. For the bones, there was higher 580/1658 ratio in OV2 compared with the C1, C2 and OV1 groups. In addition, for the incisor teeth, there was a significant increase in the carbonate/phosphate ratio [ $\nu_2\text{PO}_4^{3-}/\text{CO}_3^{2-}$  (1070/430)] for both groups, OV1 compared with C1 and OV2 compared with C2 ( $p < 0.05$ ); however, there were significant reductions of 1070/430 ratio for both groups, C2 compared with C1 and OV2 compared with OV1 ( $p < 0.05$ ). For the bones, the 1070/430 ratio was significantly greater for OV2 compared with both groups (C2 and OV1). The 1070/430 analysis results for incisor teeth and femur bones are also illustrated, respectively, in Fig. 4c, d.

The results of EDX can be seen in Fig. 5. The relationship between the main key variables can be seen in Fig. 6. For the teeth, there were negative correlations between the 1070/430 ratio band area and P concentration ( $r = -0.57$ ,  $p = 0.04$ ) in groups C1 and OV1. For the bones, there was a negative correlation between the 1070/430 ratio band area and P concentration ( $r = -0.58$ ,  $p = 0.04$ ) in groups C2 and OV2.

## Discussion

The main finding of this study was that osteoporosis induced in rats produced changes in the cortical bone and dentin, shown by the phosphate/amide I and carbonate/phosphate ratios.

For the cortical bone, the phosphate  $\nu_4$  (580  $\text{cm}^{-1}$ ) and  $\nu_1$  (960  $\text{cm}^{-1}$ ) band areas were reduced in OV1 than C1.

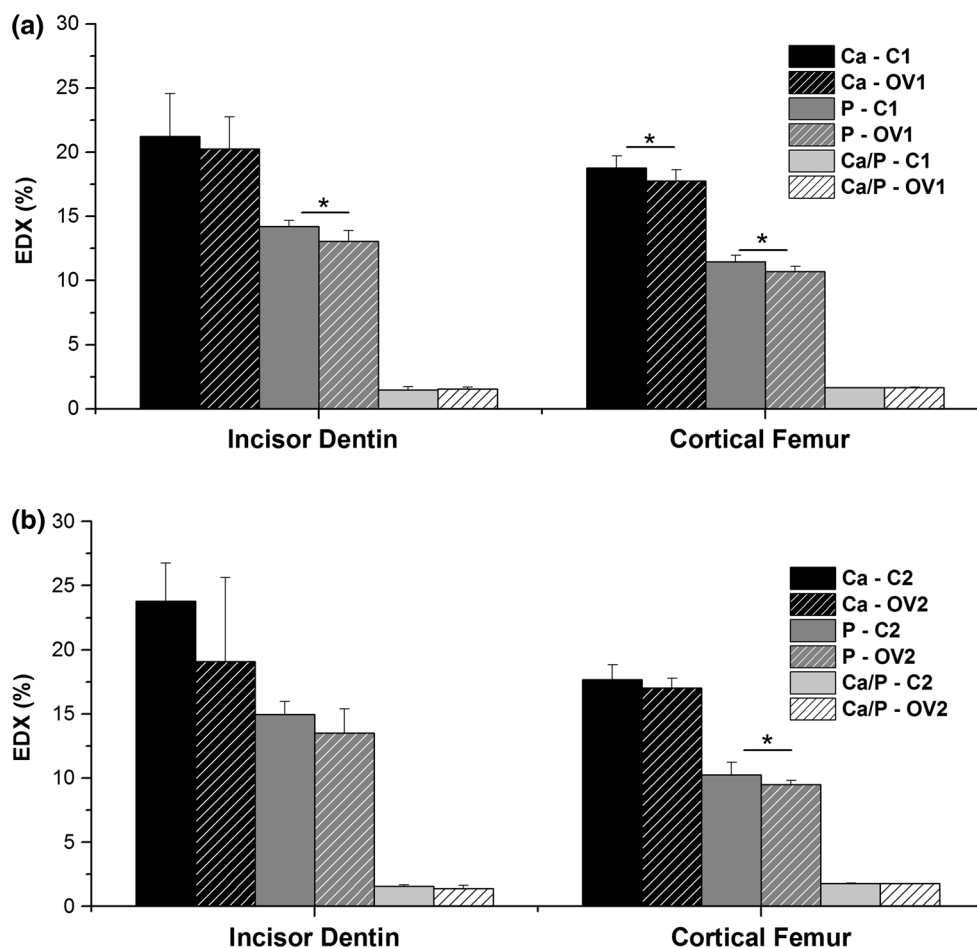


**Fig. 5** EDX analysis for incisor dentin and cortical femur in C1 and OV1 (a) and C2 and OV2 (b). For incisor dentin, there was a significant reduction in the P for OV1 vs. C1 ( $p < 0.05$ ). For the cortical

femur, there were significant reductions of the P for OV1 vs. C1 and, OV2 vs. C2, while the Ca was only reduced in OV1 vs. C1 ( $p < 0.05$ )

Moreover, the Ca and P concentrations were also reduced. These findings suggest both physicochemical and structural changes during the short-term postmenopausal period (3 months post-ovariectomy). In this context, the phosphate band area was taken as an indicator of mineral content and a marker of tissue quality [26, 27]. Therefore, there was a lower mineralization state and increased bone remodeling. Bone undergoes modeling/remodeling throughout life by activating successive phases, including resorption, reversal and formation, helping to repair microcracks and prevent the accumulation of old bone. However, in osteoporosis, there is an increased number of both osteoclasts and active bone-forming osteoblasts. This occurs due to an increased number of ongoing remodeling cycles (frequency of activation sites), reducing bone mass/strength and resistance to microdamage [28, 29].

On the other hand, interestingly, the phosphate  $\nu_4$  ( $580\text{ cm}^{-1}$ ) and  $\nu_1$  ( $960\text{ cm}^{-1}$ ) band areas significantly increased in OV2 compared with OV1, suggesting that

both physicochemical and structural changes were more considerable during the long-term postmenopausal period (6 months post-ovariectomy). These findings corroborate those obtained by phosphate/amide I ratio (960/1658) in cortical bone, also showing a significant increase in the current study. The phosphate/amide ratio indicates a different secondary structure within the collagen matrix and/or a relationship between the degree of bone maturity and the properties of the mineral crystal [26, 27]. Therefore, these significant increases found in the current study possibly occurred due to a change in the structure and mechanical properties of bones, which may be reported by collagen degradation or decreased collagen synthesis [30], degree of mineralization and overall disorder in crystallinity properties of the bone mineral (crystal size and perfection and orientation) [31, 32]. These changes in the bones are observed with aging. Furthermore, particularly, osteoporosis involves advanced bone aging and greater fracture risk. Our results indicate that in osteoporosis there was an excessive increase in the level of

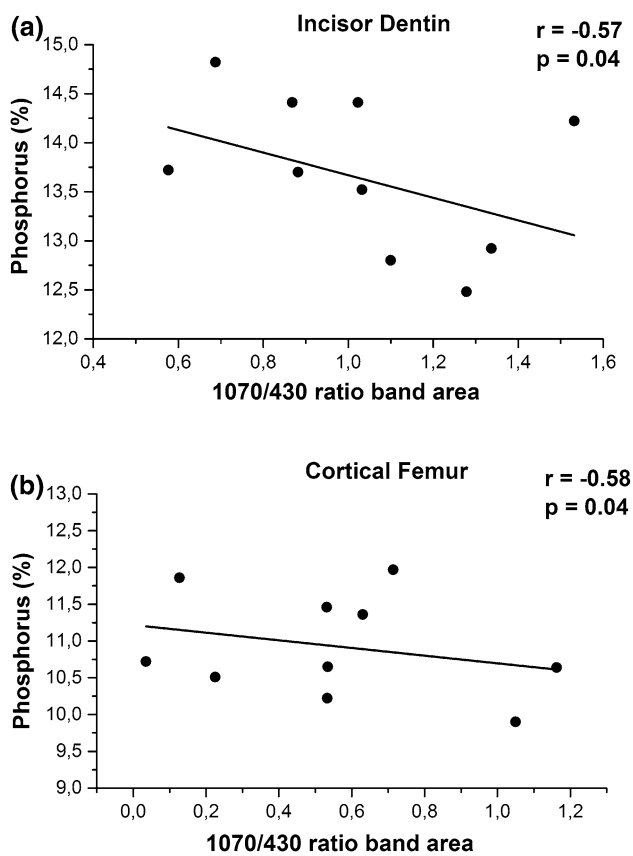


**Fig. 6** Correlations between variables. Raman shift band area as a function of EDX (in %) in 10 female Wistar rats. The regression line represents both the average of the P and 1070/430 ratio band area (a) in the incisor dentin for C1 and OV1. In addition, the regression line represents both the average of the P and 1070/430 ratio band area (b) in cortical femur for C2 and OV2. The regression was negative and statistically significant ( $p < 0.05$ ) for incisor dentin and cortical femur

bone mineralization together with an increase in stiffness of the bones, which may result in increased brittleness, requiring less energy to fracture [33]. Moreover, bone strength and quality are correlated to crystal properties, such as a larger number and size of crystals, as well as an increased degree of crystallinity. It will decrease the amount of deformation, creating and/or propagating cracks, which lead to greater bone fracture risk [33]. However, some studies [31, 34, 35] are controversial concerning mineralization levels and crystallinity properties of bone tissue due to different experimental conditions, as well as bone tissue heterogeneity and complexity [31], such as bone geometric features (size, shape and connectivity), the biological activities of cells and the bone material properties [36].

Our data about bone quality are important to estimate a fracture risk [37–39]. This fracture risk was higher in OV2 (long-term postmenopausal period). In addition, these data are reinforced by the significant increase of the carbonate/phosphate ratio (1070/430) in cortical bone for the OV2

group, as well as by the negative correlation between the P concentration and 1070/430 ratio (lower P content–larger ratio). The carbonate/phosphate ratio indicates the degree of substitution values [26, 27], but Raman spectroscopy is only able to analyze type-B carbonate substitution. Carbonate ions in a type B environment (in trivalent anionic sites) are more common compared with type A (monovalent anionic) existing in bone mineral [40]. In the current study, there is an increase in the degree of carbonation (1070/430 ratio) as a function of osteoporosis, indicating carbonate substitution for phosphate in the apatite lattice. Possibly, an increased systemic metabolic acidosis (decreasing  $\text{HCO}_3^-$  concentration) leads to an increased  $\text{H}^+$  concentration and larger bone resorption by osteoclast activation [41], delivering carbonate ( $\text{CO}_3^{2-}$ ) and hydrogen phosphate ( $\text{HPO}_4^{2-}$ ) ions to buffer the serum pH [34], leading to bone loss and structural deterioration.

Similarly to cortical bone, the dentin showed a significant increase in the phosphate/amide I and carbonate/phosphate ratios, but these changes were more considerable in OV1 (short-term postmenopausal period), while for bones these changes occurred in OV2 (long-term postmenopausal period). In parallel, there was a significant reduction in the P concentrations in dentin for OV1. Moreover, the negative correlation for dentin was found between the P and 1070/430 ratio (lower P content–larger ratio). In this context, Raman spectra, typical of the dentin, showed impure hydroxyapatite containing  $\text{CO}_3$  and  $\text{HPO}_4$ .

Moreover, for the dentin, a significant reduction of the phosphate  $\nu_2$  ( $430\text{ cm}^{-1}$ ) and carbonate ( $1070\text{ cm}^{-1}$ ) band areas for C2 compared with C1 was observed, indicating age-related changes of the teeth due to the natural aging process or type 2 osteoporosis, such as demineralization without systemic metabolic acidosis, but together with protein structural changes, shown by a reduction in the  $\text{CH}_2$  wag ( $1446\text{ cm}^{-1}$ ) band of collagen [42].

There was also a significant reduction in the proline ( $854\text{ cm}^{-1}$ ) and carbonate ( $1070\text{ cm}^{-1}$ ) band areas for OV2 compared with OV1 in dentin, but the carbonate band area was higher in OV2 compared with C2. Proline is a derivative of hydroxyproline, constituting 20% of the amino acid residues of collagen [43]. A reduced proline band area suggests changes in the organic matrix of dentin, such as degradation of the collagen structure, where possibly the stability of the collagen triple helix was affected by osteoporosis due to alterations in the degree of the hydroxylation of proline [44], resulting in altered dentin mechanical properties and, dental fragility [42]. In the current study, altered dental quality due to type 1 osteoporosis is also related to type B carbonate substitution of apatite.

Regarding other methodologies for hard tissue analysis, confocal imaging Raman microscopy reconstructs images from the Raman band, promoting an important correlation



between image and spectral analysis. Moreover, X-ray microtomography ( $\mu$ -CT) is the gold standard, and histomorphometry is usually performed to complement the data analysis [45]. Failure to include these tests in the current study is a methodological limitation. Therefore, these methods should be used in future experimental studies.

In conclusion, Raman Spectroscopy assessed compositional, physicochemical and structural changes in hard tissue (incisor dentin and cortical femur). It is a well-known fact that osteoporosis results in compositional, physicochemical and structural changes in bones, but the current study also pointed out the possible action mechanisms and bone fracture risk. Regarding teeth, our study showed that poor dental quality may also occur due to osteoporosis from the initial postmenopausal period in an animal model.

**Acknowledgements** We would like to thank the São Paulo Research Foundation (FAPESP)—Grant no. 2013/14001-9 and 2013/07276-1 (CEPOF—CEPID Program).

**Funding** This study was funded by the São Paulo Research Foundation (FAPESP)—Grant no. 2013/14001-9 and 2013/07276-1 (CEPOF—CEPID Program).

### Compliance with ethical standards

**Ethical standards** This study was approved by the Ethics Committee of the São Carlos Institute of Physics (IFSC), University of São Paulo (USP) in São Carlos, Brazil (number 08/2014). All animal procedures were performed according to the principles in the Guide for the Care and Use of Laboratory Animals.

**Conflict of interest** No competing financial interests exist.

### References

- Tu Q, Chang C (2012) Diagnostic applications of Raman spectroscopy. *Nanomedicine Nanotechnol Biol Med* 8:545–558
- Moreira LM, Silveira L Jr, Santos FV, Lyon JP, Rocha R, Zângaro RA, Villaverde AB, Pacheco MT (2008) Raman spectroscopy: a powerful technique for biochemical analysis and diagnosis. *J Spectrosc* 22:1–19
- Carden A, Morris MD (2000) Application of vibrational spectroscopy to the study of mineralized tissues (review). *J Biomed Opt* 5:259–268
- Boskey AL (2007) Mineralization of bones and teeth. *Elements* 3:385–391
- Pascart T, Cortet B, Olejnik C, Paccou J, Migaud H, Cotten A, Delannoy Y, Durling A, Hardouin P, Penel G, Falgayrac G (2016) Bone samples extracted from embalmed subjects are not appropriate for the assessment of bone quality at the molecular level using Raman spectroscopy. *Anal Chem* 88:2777–2783
- Pascart T, Falgayrac G, Migaud H, Quinchon JF, Norberciak L, Budzik JF, Paccou J, Cotten A, Penel G, Cortet B (2017) Region specific Raman spectroscopy analysis of the femoral head reveals that trabecular bone is unlikely to contribute to non-traumatic osteonecrosis. *Sci Rep* 7:97
- Buckley K, Matousek P, Parker AW, Goodship AE (2012) Raman spectroscopy reveals differences in collagen secondary structure which relate to the levels of mineralization in bones that have evolved for different functions. *J Raman Spectrosc* 43:1237–1243
- Paschalis EP, Fratzl P, Gamsjaeger S, Hassler N, Brozek W, Eriksen EF, Eriksen EF, Rauch F, Glorieux FH, Shane E, Dempster D, Cohen A, Recker R, Klaushofer K (2016) Aging versus postmenopausal osteoporosis: bone composition and maturation kinetics at actively-forming trabecular surfaces of female subjects aged 1 to 84 years. *J Bone Miner Res* 31:347–357
- Carneiro J, Leblond CP (1959) Role of osteoblasts and odontoblasts in secreting the collagen of bone and dentin, as shown by radioautography in mice given tritium-labelled glycine. *Exp Cell Res* 18:291–300
- Wang Z, McCauley LK (2011) Osteoclasts and odontoclasts: signaling pathways to development and disease. *Oral Dis* 17:129–142
- Yokose S, Zhungfeng C, Tajima Y, Fujieda K, Katayama I, Katayama T (1998) The effects of estrogen deficiency on glycosylation of odontoblasts in rats. *J Endod* 24:645–647
- Kim M, Yang WK, Baek J, Kim JJ, Kim WK, Lee YK (2005) The effect of estrogen deficiency on rat pulpodentinal complex. *J Korean Acad Conserv Dent* 30:402–408
- Xu T, Yan M, Wang Y, Wang Z, Xie L, Tang C, Zhang G, Yu J (2014) Estrogen deficiency reduces the dentinogenic capacity of rat lower incisors. *Mol Histol* 45:11–19
- Lu Y, Jin L, Lei G, Fu Y, Wang Y, Yu J (2016) Estrogen-mediated dental tissue regeneration. *Histol Histopathol* 31:1281–1289
- Wang Y, Yan M, Yu Y, Wu J, Yu J, Fan Z (2013) Estrogen deficiency inhibits the odonto/osteogenic differentiation of dental pulp stem cells via activation of the NF- $\kappa$ B pathway. *Cell Tissue Res* 352:551–559
- Schour I, Steadman SR (1935) The growth pattern and daily rhythm of the incisor of the rat. *Anat Rec* 63:325–333
- Bhaskar SN (1953) Growth pattern of the rat mandible from 13 days insemination age to 30 days after birth. *Am J Anat* 92:1–53
- Jeffcoat M (2005) The association between osteoporosis and oral bone loss. *J Periodontol* 76:2125–2132
- Paolillo FR, Romano RA, de Matos L, Rodrigues PGS, Panhóca VH, Martin AA, Soares LE, de Castro Neto JC, Bagnato VS (2016) Fluorescence spectroscopy of teeth and bones of rats to assess demineralization: in vitro, in vivo and ex vivo studies. *J Photochem Photobiol B* 165:291–297
- Raisz LG (1999) Physiology and pathophysiology of bone remodeling. *Clin Chem* 45:1353–1358
- Riggs BL, Khosla S, Melton LJ (1998) A unitary model for involutional osteoporosis: estrogen deficiency causes both type I and type II osteoporosis in postmenopausal women and contributes to bone loss in aging men. *J Bone Miner Res* 13:763–773
- McCreadie BR, Morris MD, Chen TC, Rao DS, Finney WF, Widjaja E, Goldstein SA (2006) Bone tissue compositional differences in women with and without osteoporotic fracture. *Bone* 39:1190–1195
- Inzana JA, Maher JR, Takahata M, Schwarz EM, Berger AJ, Awad HA (2013) Bone fragility beyond strength and mineral density: Raman spectroscopy predicts femoral fracture toughness in a murine model of rheumatoid arthritis. *J Biomech* 46:723–730
- Richards-Kortum R, Sevick-Muraca E (1996) Quantitative optical spectroscopy for tissue diagnosis. *Annu Rev Phys Chem* 47:555–606
- Adabbo M, Paolillo FR, Bossini PS, Rodrigues NC, Bagnato VS, Parizotto NA (2016) Effects of low-level laser therapy applied before treadmill training on recovery of injured skeletal muscle in Wistar rats. *Photomed Laser Surg* 34:187–193

26. Goodyear SR, Gibson IR, Skakle JMS, Wells RPK, Aspden RM (2009) A comparison of cortical and trabecular bone from C57 Black 6 mice using Raman spectroscopy. *Bone* 44:899–907
27. Morris MD, Mandair GS (2011) Raman assessment of bone quality. *Clin Orthop Relat Res* 469:2160–2169
28. Lerner UH (2006) Bone remodeling in post-menopausal osteoporosis. *J Dent Res* 85:584–595
29. Hadjidakis DJ, Androulakis II (2006) Bone remodeling. *Ann N Y Acad Sci* 1092:385–396
30. Matsumoto Y, Mikuni-Takagaki Y, Kozai Y, Miyagawa K, Naruse K, Wakao H, Kawamata R, Kashima I, Sakurai T (2009) Prior treatment with vitamin K2 significantly improves the efficacy of risedronate. *Osteoporos Int* 20:1863–1872
31. Paschalis EP, Betts F, DiCarlo E, Mendelsohn R, Boskey AL (1997) FTIR microspectroscopic analysis of human iliac crest biopsies from untreated osteoporotic bone. *Calcif Tissue Int* 61:487–492
32. Kazanci M, Roschger P, Paschalis EP, Klaushofer K, Fratzl P (2006) Bone osteonal tissues by Raman spectral mapping: orientation–composition. *J Struct Biol* 156:489–496
33. Davison KS, Siminoski K, Adachi JD, Hanley DA, Goltzman D, Hodsmann AB, Robert J, Kaiser S, Olszynski WP, Papaioannou A, Ste-Marie LG, Kendler DL, Tenenhouse A, Brown JP (2006) Bone strength: the whole is greater than the sum of its parts. In *Semin Arthritis Rheum* 36:22–31
34. Yerramshetty JS, Lind C, Akkus O (2006) The compositional and physicochemical homogeneity of male femoral cortex increases after the sixth decade. *Bone* 39:1236–1243
35. Boskey AL, Spevak L, Paschalis E, Doty SB, McKee MD (2002) Osteopontin deficiency increases mineral content and mineral crystallinity in mouse bone. *Calcif Tissue Int* 71:145–154
36. Faibish D, Ott SM, Boskey AL (2006) Mineral changes in osteoporosis: a review. *Clin Orthop Relat Res* 443:28–38
37. Yerramshetty JS, Akkus O (2008) The associations between mineral crystallinity and the mechanical properties of human cortical bone. *Bone* 42:476–482
38. Buckley K, Kerns JG, Vinton J, Gikas PD, Smith C, Parker AW, Matousek P, Goodship AE (2015) Towards the in vivo prediction of fragility fractures with Raman spectroscopy. *J Raman Spectrosc* 46:610–618
39. Paschalis EP, Gamsjaeger S, Dempster D, Jorgetti V, Borba V, Boguszewski CL, Klaushofer K, Moreira CA (2017) Fragility fracture incidence in chronic obstructive pulmonary disease (COPD) patients associates with nanoporosity, mineral/matrix ratio, and pyridinoline content at actively bone-forming trabecular surfaces. *J Bone Miner Res* 32:165–171
40. Rey C, Collins B, Goehl T, Dickson IR, Glimcher MJ (1989) The carbonate environment in bone mineral: a resolution-enhanced Fourier transform infrared spectroscopy study. *Calcif Tissue Int* 45:157–164
41. Meghji S, Morrison MS, Henderson B, Arnett TR (2001) pH dependence of bone resorption: mouse calvarial osteoclasts are activated by acidosis. *Am J Physiol Endocrinol Metab* 280:E112–E119
42. Ager JW, Nalla RK, Balooch G, Kim G, Pugach M, Habelitz S, Marshall GW, Kinney JH, Ritchie RO (2006) On the increasing fragility of human teeth with age: a deep-UV resonance Raman study. *J Bone Miner Res* 21:1879–1887
43. Weinstock M, Leblond CP (1974) Synthesis, migration, and release of precursor collagen by odontoblasts as visualized by radioautography after [<sup>3</sup>H] proline administration. *J Cell Biol* 60:92–127
44. Rosenbloom J, Harsch M, Jimenez S (1973) Hydroxyproline content determines the denaturation temperature of chick tendon collagen. *Arch Biochem Biophys* 158:478–484
45. Paolillo AR, Paolillo FR, Silva AMH, Reiff RBM, Bagnato VS, Alves JM (2015) Effects of infrared laser on the bone repair assessed by X-ray microtomography ( $\mu$ ct) and histomorphometry. In: *Proceedings of SPIE biophotonics, South America, Rio de Janeiro, 9531 (95313N-1–95313N-7)*